

Channel Characteristics Analysis of 60 GHz Wireless Communications in Staircase Environments

Cuiping Zhang¹, Jian Sun¹, Yu Liu², Wensheng Zhang¹, and Cheng-Xiang Wang^{3,4}

¹Shandong Provincial Key Lab of Wireless Communication Technologies,
School of Information Science and Engineering, Shandong University, Qingdao, Shandong, 266237, China.

²School of Microelectronics, Shandong University, Jinan, Shandong, 250101, China.

³National Mobile Communications Research Laboratory,
School of Information Science and Engineering, Southeast University, Nanjing, Jiangsu, 210096, China.

⁴Purple Mountain Laboratories, Nanjing, Jiangsu, 211111, China.

Email: 201812598@mail.sdu.edu.cn

{sunjian, yuliu, zhangwsh}@sdu.edu.cn, chxwang@seu.edu.cn

Abstract—The fifth generation mobile communication (5G) is being commercialized. As two pivotal technologies of 5G, millimeter-wave (mmWave) and massive multiple-input multiple-output (MIMO) have attracted widespread attention. Many measurements and simulations have been conducted in various indoor scenarios combining these two technologies. Nevertheless, staircase environments are rarely involved. This paper investigates the channel characteristics with MIMO technology at 60 GHz frequency band in a staircase environment. A simulation campaign with 8×16 and 1×128 MIMO system is carried out. In case of 8×16 MIMO system, the change tendency of average power delay profile (APDP) with the movement of receiver (Rx) at different transmitter (Tx) heights is studied. The large-scale parameters (LSPs) such as path loss, shadow fading (SF), root-mean-square (RMS) delay spread (DS) and angular spread (AS), Ricean K -factor (KF) are also analyzed. Then the inter-parameter correlation and decorrelation distance for above LSPs are extracted. In addition, the spatial correlation coefficient between antenna elements along 64-element linear array with disparate Tx heights is also demonstrated. The channel parameter characteristics studied in this paper will provide an insight into the design of future wireless communication system for staircase environment.

Index Terms—Ray tracing, mmWave, MIMO, LSPs, spatial correlation

I. INTRODUCTION

With the development of wireless communications, more and more wireless devices and applications connect to mobile networks, giving rise to a rapid increase of data. In order to meet the needs of users, 5G technology comes into being, and it will be commercialized around 2020. Compared with previous generations of mobile communication technologies, 5G towards higher data rate, higher system capacity and lower network delay. Massive MIMO and mmWave are two most promising technologies of 5G. With smaller wavelength, the mmWave frequency is an excellent choice to satisfy the demands of massive MIMO [1]. Researches on the sixth generation mobile communication (6G) are being carried out, it will be in a much higher frequency band. Massive MIMO technology is likely to provide important technical support for the 6G. Therefore, research on massive MIMO technology at

mmWave bands still has a great significance to future wireless communications.

From the existing literatures, massive MIMO technology and mmWave have been used to conduct numerous researches in a variety of indoor scenarios recent years. In particular, since 60 GHz can provide up to 7 GHz unlicensed spectrum, it has the most potential to develop multigigabit wireless communication systems [2], and has gained extensive concern. In [3], the received power and fading characteristics were studied in L-shaped and T-shaped corridor environments based on ray tracing method at 60 GHz. Vertically polarized omnidirectional antennas were used in [4] to investigate the channel characteristics such as RMS DS, path loss and received power in a living room at 60 GHz band. In [5], simulation and uniform virtual array (UVA) based channel measurement were implemented in an office environment, the small-scale channel properties like power delay profile (PDP) and power angular spectrum were analyzed. Similarly, the combination of massive MIMO technology and mmWave has attracted a lot of attention. Massive MIMO was applied for measurement and simulation at around 26 GHz in a center hall environment to investigate the channel characteristics [6]. The influence of spatial correlation between antenna elements on channel capacity was studied in an open office environment based on 28 GHz MIMO channel measurement [7]. In the same indoor office environment, combined with massive MIMO technology, experimental channel measurements were conducted at 11, 16, 28, and 38 GHz bands [8].

As a vital part of the floor building, staircase plays an important role in our daily life as well as emergency situations [9]. It is favourable for the future communication system deployment and design to study the wireless channel characteristics in staircase environments. In [9], measurements and simulation at 2.4 GHz with different antenna polarization modes were carried out to investigate the propagation characteristics in a staircase. A novel path loss model was proposed under indoor staircase environment at 2.6 GHz [10], [11]. Both two papers considered the influence of antenna height. In addition, [10] premeditated the impact of beams in some stairs,

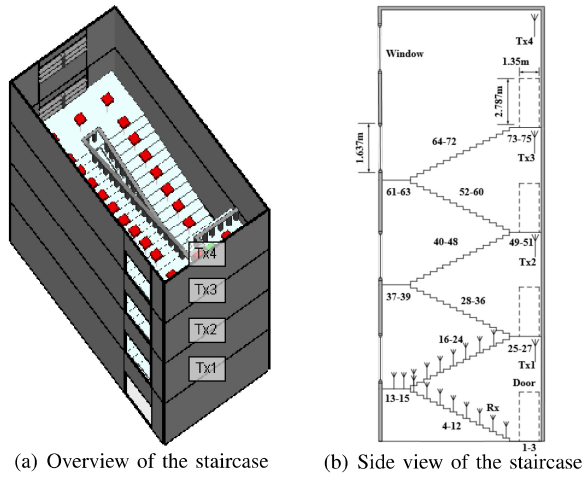


Fig. 1. Staircase environment model

which makes it more validly and pragmatic to expound the channel characteristics in the indoor staircase environments. A wearable MIMO technology is used to present the channel characteristics in the stairwell environment at 3 GHz, 4 GHz and 5 GHz bands [12]. Simulation at 60 GHz with single antenna was conducted to investigate the channel clustering and analysis in a staircase environment. However, there is almost no measurements or simulations combine 60 GHz with MIMO technology to focus on the channel characteristics in staircase environments. For this reason, based on [13], MIMO technology is considered in this paper. What is more different is that the staircase environment in this paper has one more floor and the staircase handrails are continuous. In addition, the channel characteristics we analyzed are not the same.

The remainder of this paper is organized as follows. The configuration of the simulation environment is described in Section II. An overview of the channel characteristics such as APDP, path loss, SF, RMS DS and AS, KF, inter-parameter correlation and decorrelation distance, spatial correlation, as well as the analysis of simulation results are presented in Section III. Finally, we draw the conclusions in Section IV.

II. STAIRCASE SIMULATION

A. Modeling of the Staircase Environment

For the sake of saving time and cost, a 3D ray tracing simulator called Wireless InSite (WI) is used to execute the simulation of a staircase wireless network. Based on consistent diffraction theory (UTD) and geometric diffraction theory (GTD), the software adopts ray tracing method to establish the propagation model. It can realize accurate and effective wireless propagation prediction and channel characteristic prediction in any complex environments.

In this study, the simulation scenario, shown in Fig. 1, is a portion of an office building. We assumed that the simulation is performed in a closed environment with a ceiling and without other obstacles. The staircase scenario consists of walls, windows, guardrails, stair steps, stair railings, floor,

TABLE I
PARAMETERS FOR MATERIALS AT 60 GHz.

Materials	Relative permittivity (F/m)	Electric conductivity (S/m)	Thickness (m)
Concrete	5.31	0.897	0.300
Dry wall	2.94	0.210	0.013
Glass	6.27	0.567	0.003
Ceiling board	1.50	0.059	0.009
Floorboard	3.66	1.113	0.030

TABLE II
ENVIRONMENTAL CONDITIONS.

Tx index	LOS position index	NLOS position index
1	Rx 1-14	Rx 15-75
2	Rx 14-38	Rx 1-13, Rx 39-75
3	Rx 38-62	Rx 1-37, Rx 63-75
4	Rx 55-75	Rx 1-54

and ceiling. Fig. 1(a) shows an overview of the simulation environment in WI, the side view of the staircase is illustrated as Fig. 1(b).

The length of the staircase environment is 7.6 m, the width is 3.6 m and the height is 21.098 m. Four floors are contained in the scenario, each floor consists of one platform and two flights of stairs. There are 16 steps in every flight of stairs. The length, width and height of each step are 1.62 m, 0.54 m, 0.15 m, respectively. Each floor has a doorway. In addition, there is a window on the walls of each floor equipped with a metal guardrail. The stair steps are made of concrete, the stair railings and guardrails are both made of ideal metal. The electromagnetic parameters of all materials in the staircase adopt the specific parameters in the 60 GHz frequency band provided by the WI material library as shown in Table I. Moreover, the roughness effect of the materials is also taken into account, so the lambertian scattering model is added in the environment to ensure the authenticity and effectiveness of the simulation environment. Five reflections, one diffraction, and one transmission are used in this simulation [14], and two reflections are set under the diffuse scattering.

B. Simulation System

Four Tx's are placed in the scenario, as shown in Fig. 1, each is located on the top of the floor, mounted on the wall without window. The Rx with 1.5 m tall moves step by step along the stair steps, total 75 positions are measured. Table II lists the scenario conditions about line-of-sight (LOS) and none-line-of-sight (NLOS). MIMO antenna array is utilized to send and receive signals at Tx and Rx. We use two types of antenna array at Tx side for simulation. One is a 16-element uniform planar array with ten wavelength spacing, the other is a cross-shaped linear array of 128-element with half a wavelength. The uniform planar array is composed of 4×4 elements, while the linear array consists of two 64-element uniform linear arrays that parallel and perpendicular to the ground. The Rx side accordingly uses a 4×2 planar array with eight wavelength

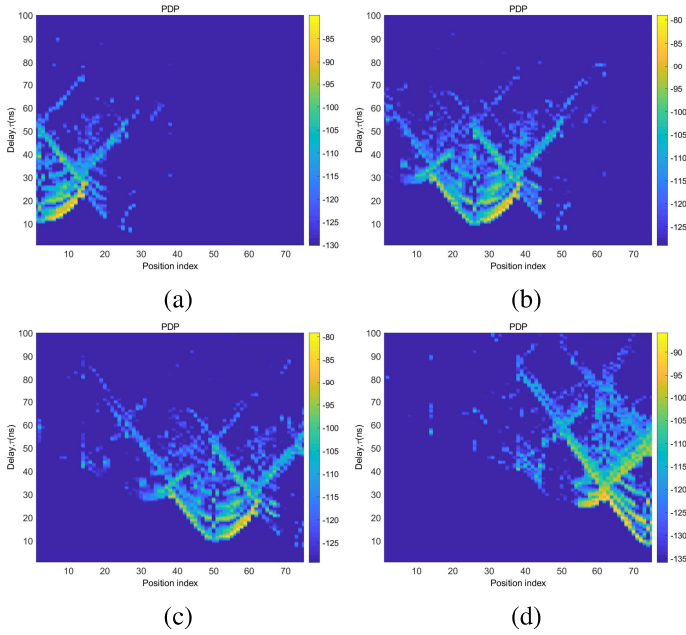


Fig. 2. APDPs with the movement of Rx at four different Tx heights. (a) Tx1. (b) Tx2. (c) Tx3. (d) Tx4

spacing and a single antenna. All of the antenna elements are vertical polarization omni-directional antenna. The transmit power is 30 dBm.

III. CHANNEL CHARACTERIZATION AND ANALYSIS

A. Power Delay Profile

PDP reflects the distribution of the received power at different time delays. It can be calculated based on the channel impulse response (CIR) $h(\tau)$ which is derived by using the inverse Fourier transform on channel transfer function (CTF) \mathbf{H} . The CTF can be calculated by the following formula.

$$\mathbf{H}(f_k, i, j) = \sum_{l=1}^L \alpha_l e^{j\phi_l} e^{-j2\pi f_k \tau_l}, \quad (1)$$

where f_k denotes the k^{th} frequency point. i and j represent the i^{th} and j^{th} transmit and receive antenna elements, respectively. α_l , ϕ_l , and τ_l are the amplitude, phase, and delay of the l^{th} multipath component (MPC), respectively. $h(\tau)$ can be obtained as

$$h(\tau_n, i, j) = \frac{1}{\|w\| \sqrt{N_{sc}}} \sum_{k=-N_{sc}/2}^{N_{sc}/2-1} w(k) \mathbf{H}(f_k, i, j) e^{\frac{j2\pi k \tau_n}{N_{sc}}}, \quad (2)$$

where $N_{sc} = 1024$ is the number of sub-carriers. w denotes the window function, Kaiser-Bessel Window is used here to suppress side lobes.

The APDP can be obtained by averaging PDPs over all sub-channels at each pair of Tx and Rx [15].

$$APDP(\tau_n) = \frac{1}{N_T N_R} \sum_{i=1}^{N_T} \sum_{j=1}^{N_R} |h(\tau_n, i, j)|^2, \quad (3)$$

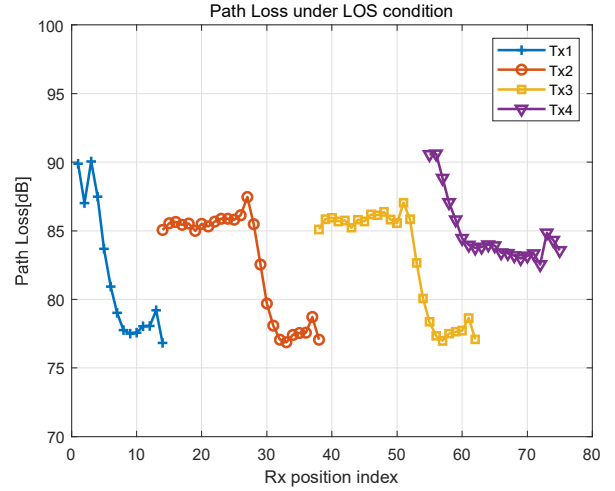


Fig. 3. Path loss with the movement of Rx at four different Tx heights.

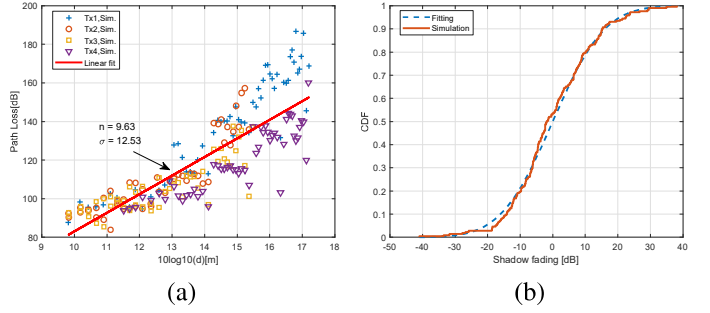


Fig. 4. Path loss and shadow fading. (a) Path loss under the NLOS scenario. (b) CDF of shadow fading for the NLOS scenario.

where N_T and N_R are the number of antenna elements at Tx and Rx, respectively.

Fig. 2 shows the change of APDP with the movement of Rx at different Tx heights. In order to clearly see the variation of APDP with the movement of Rx, we first align the PDP peaks of each pair of antenna elements. It can be seen clearly that the multipath propagation is very rich in the staircase scenario. In addition, as can be seen from the figure, there is always a LOS path with higher power and several reflection paths with relatively low power in the LOS scenario. While in the case of NLOS scenario, with the movement of Rx, only a few diffracted and multi-order reflected rays can reach the receiver with less power.

B. Path Loss and Shadow Fading

Path loss is an important large-scale parameter (LSP) that can be used to characterize the propagation loss in channel propagation, the common logarithmic distance path loss model can be described as follow [16]

$$PL(d) = PL_0 + 10n \log_{10} \left(\frac{d}{d_0} \right) + X_s, \quad (4)$$

where PL_0 is the path loss at the reference distance $d_0 = 1m$, n is the path loss exponent. The d in NLOS scenario is denoted

by the walking distance of Rx moves up or down from the floor where Tx located [17]. X_s is generally modeled as a zero-mean Gaussian process with a standard deviation σ_s . The path loss can be determined by the APDP or CTF as follows

$$PL = -10 \log_{10} \left(\sum_{n=0}^{N_{sc}-1} APDP(\tau_n) \right) \\ = -10 \log_{10} \left(\frac{1}{N_T N_R N_{sc}} \sum_{i=1}^{N_T} \sum_{j=1}^{N_R} \sum_{k=1}^{N_{sc}} |\mathbf{H}(f_k, i, j)|^2 \right). \quad (5)$$

As shown in Fig. 3, in the case of LOS scenario, when Rx is close to Tx, the path loss almost unchanged. However, when Rx is far from Tx, the path loss decreases first and then tends to be stable. Least linear square fitting is performed on the simulation data to obtain the path loss exponent. Fig. 4(a) shows the scatter plots of the path loss and its linear fit with logarithmic distance in NLOS scenario. The path loss exponent $n = 9.63$ and the standard deviation $\sigma_s = 12.53$. It is worth noting that the path loss exponent n is higher than the value of the same type staircase in [18], which is because of our staircase scenario has more stair steps, and each floor has a window equipped with a metal guardrail, the staircase structure is relatively complex. The cumulative distribution function (CDF) of the SF under the NLOS scenario is shown in Fig. 4(b), which fits well with the log-normal distribution.

C. RMS Delay Spread and RMS Angle Spread

The RMS DS is most commonly used to quantify the dispersion of wideband multipath channels in delay domain, it can be expressed by [16]

$$\sigma_{DS} = \sqrt{\frac{\sum_{l=1}^L P(\tau_l) \cdot \tau_l^2}{\sum_{l=1}^L P(\tau_l)} - \left(\frac{\sum_{l=1}^L P(\tau_l) \cdot \tau_l}{\sum_{l=1}^L P(\tau_l)} \right)^2}, \quad (6)$$

where $P(\tau_l)$ is the power of the l^{th} MPC.

The RMS AS reflects the power dispersion in angular domain, which can be calculated as

$$\sigma_{AS} = \sqrt{\frac{\sum_{l=1}^L P(\tau_l) \cdot \psi_l^2}{\sum_{l=1}^L P(\tau_l)} - \left(\frac{\sum_{l=1}^L P(\tau_l) \cdot \psi_l}{\sum_{l=1}^L P(\tau_l)} \right)^2}, \quad (7)$$

where ψ_l denotes the azimuth or elevation angle of arrival or departure of the l^{th} MPC. Fig. 5(a)-(e) show the CDF plots of the RMS AS and DS with all Tx heights. Four angular spreads are contained in RMS AS, such as azimuth angular spread of departure (ASD), elevation angular spread of departure (ESD), azimuth angular spread of arrival (ASA), and elevation angular spread of arrival (ESA). All of them are fitted by a log-normal distribution. The azimuth and elevation angular spreads are mainly in the range of 32° - 100° and 3° - 32° .

D. Ricean K-factor

The KF reflects the power difference between LOS and NLOS components, which is defined as the ratio of the power

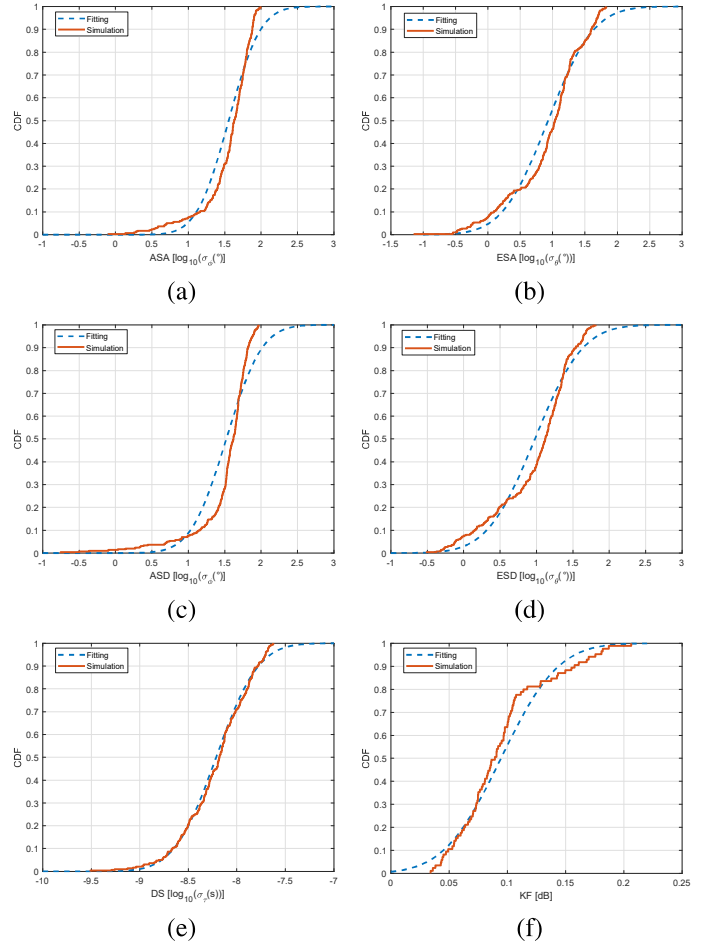


Fig. 5. (a) CDF of ASA. (b) CDF of ESA. (c) CDF of ASD. (d) CDF of ESD. (e) CDF of DS. (f) CDF of KF.

of direct path to the sum power of other paths. It can be calculated as

$$KF = \frac{P_{LOS}}{P - P_{LOS}}, \quad (8)$$

where P_{LOS} is the power of the direct path, P denotes the sum power of all paths. The CDF plot of KF is shown as Fig. 5(f). It can be observed that the values of KF are less than 1. When the probability gets to 1, the value of KF is only 0.2, which demonstrates that the propagation of the rays are mainly reflection and diffraction in the LOS scenarios, while the direct component is relatively small.

E. Inter-parameter Correlation.

The inter-parameter correlation reflects the dependence between different LSPs including DS, four angular spreads, KF, and SF. The correlation between any two different LSPs can be calculated through the Pearson product-moment correlation coefficient, as follows [18].

$$\rho_{X,Y} = \frac{E[(X - \mu_X)(Y - \mu_Y)]}{\sigma_X \sigma_Y}, \quad (9)$$

TABLE III
CORRELATION COEFFICIENT FOR LSPs

LSPs	DS	ASA	ESA	ASD	ESD	KF	SF
DS	1.00	0.46	0.77	0.59	0.63	-0.59	0.06
ASA	0.47	1.00	0.30	-0.05	0.15	-0.73	-0.23
ESA	0.47	0.33	1.00	0.40	0.86	-0.51	0.00
ASD	0.35	0.11	0.49	1.00	0.31	-0.33	0.33
ESD	0.00	0.02	0.79	0.03	1.00	-0.35	0.02
KF	N/A	N/A	N/A	N/A	N/A	1.00	0.13
SF	0.11	0.28	0.19	0.10	0.33	N/A	1.00

LOS condition NLOS condition

TABLE IV
DECORRELATION DISTANCE FOR LSPs

	DS	ASA	ESA	ASD	ESD	KF	SF
LOS	3.73	5.04	1.44	2.10	0.08	1.70	0.33
NLOS	7.29	0.04	1.15	7.14	3.44	N/A	7.14

where X and Y represent two different LSPs, respectively. μ and σ are the mean value and the standard deviation of the LSP.

The correlation coefficients of LSPs are summarized in Table III. The upper triangle and lower triangle areas in the table correspond to the values of the LOS scenario and the NLOS scenario, respectively. The KF has a negative correlation with DS and AS. Due to the special structure of the staircase scenario, the propagation of rays is mainly reflection and diffraction. Therefore, the value of KF is relatively low, which leads to high values for the DS and AS. In addition, DS and AS basically have a positive correlation with each other in both LOS and NLOS scenario. The SF also has a positive correlation with DS and AS in the NLOS scenario.

F. Decorrelation Distance

The decorrelation distance d_λ in meter describes the auto-correlation of LSP when Rx moves a certain distance. It can be calculated by formula (9), which is expressed as

$$\rho_{\Delta d} = \frac{E[(X_d - \mu_X)(X_{d+\Delta d} - \mu_X)]}{\sigma_X^2}, \quad (10)$$

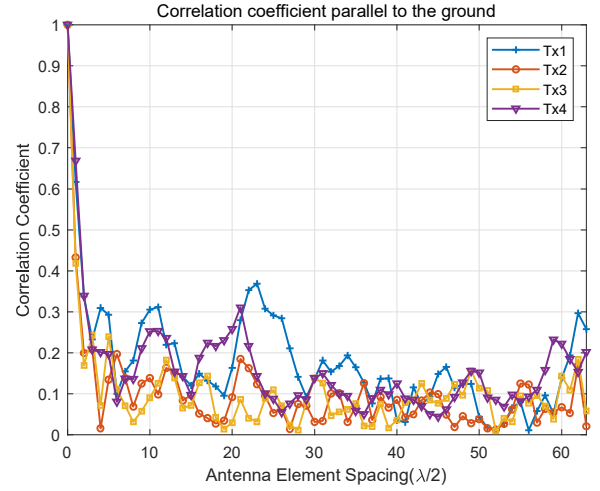
$$d_\lambda = \operatorname{argmax}_{\Delta d > 0} (|\rho_{\Delta d}| < T), \quad (11)$$

where Δd is the distance interval between two Rx positions. E represents the expectation operation. T is the threshold with the value e^{-1} [19], [20].

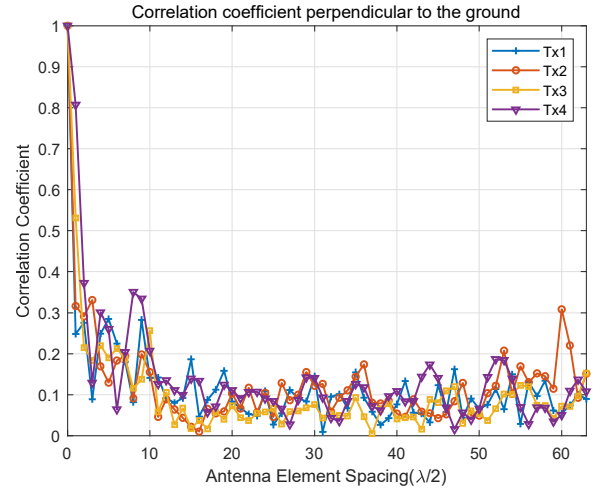
The results of decorrelation distance are presented in Table IV. The values of ESD in the LOS scenario as well as the values of ASA in the NLOS scenario are very small, which implies that as the Rx moves, these parameters themselves are nearly uncorrelated. The values of DS, ASD, and SF in the NLOS scenario are comparatively high, which means that they are highly self-correlated.

G. Spatial Correlation

Spatial correlation is a key parameter which should be taken into account in the MIMO system [21]. It has a great influence



(a) 64-element uniform linear array parallel to the ground.



(b) 64-element uniform linear array perpendicular to the ground.

Fig. 6. Correlation coefficient of cross-shaped linear antenna array.

on the performance of MIMO system. Here, we research the spatial correlation based on a 1×128 MIMO system. The correlation coefficient between antenna array elements at each Rx can be described by the following formula.

$$\begin{aligned} A_c(\Delta s) &= E[H^*(s)H(s + \Delta s)], \\ &= \frac{1}{N_e - 1} \sum_{s=1}^{N_e} H(s + \Delta s)H^*(s), \end{aligned} \quad (12)$$

where Δs represents the antenna element spacing, $(\cdot)^*$ is the complex conjugate. N_e denotes the number of antenna elements. H denotes the channel coefficient between transmitting antenna element and receiving antenna element in delay domain. Then the normalization for each Rx to get the final spatial correlation coefficient.

$$\tilde{A}_c(\Delta s) = \frac{A_c(\Delta s)}{A_c(\Delta s = 0)}. \quad (13)$$

Fig. 6(a) and (b) illustrate the correlation coefficient of two kinds of 64-element linear antenna arrays that parallel and perpendicular to the ground at Tx side, respectively. The variation of correlation coefficient between different antenna element spacings can be seen, as well as the difference among various Tx heights. It is clear that with the increasing of antenna element spacing, the correlation coefficient between antenna elements shows a trend of decreasing fluctuation. In addition, it is noted that the correlation coefficient of linear antenna array which is perpendicular to the ground does not change significantly between different Tx heights. Whereas for the linear antenna array parallel to the ground, when the antenna element spacing is between 2λ and 30λ , the correlation coefficients of Tx1 and Tx4 are greater than those of Tx2 and Tx3. Moreover, the correlation coefficients fluctuate more distinctly. Therefore, in the design of the antenna array, the influence of Tx height and the placement of the antenna element on the spatial correlation should be fully considered.

IV. CONCLUSIONS

This paper presents a simulation research in staircase environment with MIMO technology at 60 GHz. We mainly investigate the LSPs channel characteristics. A 8×16 MIMO system is used to study the change tendency of APDP with the movement of Rx at different Tx heights, the results show that there is always a LOS path with higher power and several reflection paths with lower power in the LOS scenario. The path loss exponent is also extracted from the simulation data. Due to the complexity of our staircase environment, the value of n is higher than that of staircase of the same type. In addition, the CDF plots of SF, DS, KF, and four angular spreads are fitted well by log-normal distribution. The inter-parameter correlation and decorrelation distance about LSPs are also analyzed, the results show that the KF has a negative correlation with DS and AS, since the propagation of the rays are mainly reflection and diffraction which results in a low value of KF and high values of DS and AS. The DS, ASD, and SF are highly self-correlated in the NLOS scenario. Finally, the spatial correlation between antenna elements with two types 64-element linear array is conducted, the results indicate that the placement of antenna array elements should be fully considered for different Tx heights. The results expound here may give a reference for the design of future MIMO communication systems.

ACKNOWLEDGMENT

This work was supported by the National Key R&D Program of China under Grant 2018YFB1801101, the National Natural Science Foundation of China (NSFC) under Grant 61771293 and 61960206006, the Shandong Natural Science Foundation under Grant ZR2019BF040, the Frontiers Science Center for Mobile Information Communication and Security, the High Level Innovation and Entrepreneurial Research Team Program in Jiangsu, the High Level Innovation and Entrepreneurial Talent Introduction Program in Jiangsu, the Research Fund of National Mobile Communications Research

Laboratory, Southeast University, under Grant 2020B01, the Fundamental Research Funds for the Central Universities under Grant 2242020R30001, the Huawei Cooperation Project, the EU H2020 RISE TESTBED2 project under Grant 872172, and the Taishan Scholar Program of Shandong Province.

REFERENCES

- [1] T. S. Rappaport *et al.*, "Millimeter wave mobile communications for 5G cellular: It will work!," *IEEE Access*, vol. 1, pp. 335–349, May. 2013.
- [2] A. Maltsev, R. Maslennikov, A. Sevastyanov, A. Khoryaev, and A. Lomayev, "Experimental investigations of 60 GHz WLAN systems in office environment," *IEEE J. Sel. Areas Commun.*, vol. 27, no. 8, pp. 1488–1499, Oct. 2009.
- [3] D. Sun, Y. Liu and S. Li, "Simulation and Analysis of 60 GHz Millimeter-Wave Propagation Characteristics in Corridor Environment," in *Proc. ICMMT'18*, Chengdu, May. 2018, pp. 1–3.
- [4] S. Li, Y. Liu, L. Lin, D. Sun, S. Yang and X. Sun, "Simulation and Modeling of Millimeter-Wave Channel at 60 GHz in Indoor Environment for 5G Wireless Communication System," in *Proc. ICCEM'18*, Chengdu, Mar. 2018, pp. 1–3.
- [5] A. Zhou, J. Huang, J. Sun, Q. Zhu, C. Wang and Y. Yang, "60 GHz channel measurements and ray tracing modeling in an indoor environment," in *Proc. WCSP'17*, Nanjing, Oct. 2017, pp. 1–6.
- [6] B. Ai *et al.*, "On Indoor Millimeter Wave Massive MIMO Channels: Measurement and Simulation," *IEEE J. Sel. Areas Commun.*, vol. 35, no. 7, pp. 1678–1690, Jul. 2017.
- [7] A. Xia *et al.*, "28 GHz MIMO Channel Capacity Analysis for 5G Wireless Communication Systems," in *Proc. ISAPE'18*, Hangzhou, China, Dec. 2018, pp. 1–4.
- [8] J. Huang, C. Wang, R. Feng, J. Sun, W. Zhang and Y. Yang, "Multi-Frequency mmWave Massive MIMO Channel Measurements and Characterization for 5G Wireless Communication Systems," *IEEE J. Sel. Areas Commun.*, vol. 35, no. 7, pp. 1591–1605, Jul. 2017.
- [9] S. Y. Lim, Z. Yun, J. M. Baker, N. Celik, H. Youn and M. F. Iskander, "Propagation Modeling and Measurement for a Multifloor Stairwell," *IEEE AWPL'09*, vol. 8, pp. 583–586, May. 2009.
- [10] Y. Yu, Y. Liu, W. Lu, and H. Zhu, "path loss model with antenna height dependency under indoor stair environment," *INT J Antennas Propag.*, vol. 2014, pp 1–6, Jul. 2014.
- [11] Y. Yu, Y. Liu, W. Lu, and H. Zhu, "Antenna-Height-Dependent Path Loss Model and Shadowing Characteristics Under Indoor Stair Environment at 2.6 GHz," *IEEE Trans. Elect. Electron. Eng.*, vol. 10, no. 5, pp.498–502, Jun. 2015.
- [12] P. A. Catherwood and W. G. Scanlon, "Multiple antenna channel characterisation for wearable devices in an indoor stairwell environment," *IET Microwaves, Antennas & Propag.*, vol. 12, no. 6, pp. 920–924, Feb. 2018.
- [13] Y. Yang, J. Sun, W. Zhang, C. Wang and X. Ge, "Ray Tracing Based 60 GHz Channel Clustering and Analysis in Staircase Environment," in *Proc. IEEE GCC'17*, Singapore, Dec. 2017, pp. 1–5.
- [14] G. E. Athanasiadou, A. R. Nix and J. P. McGeehan, "A ray tracing algorithm for microcellular and indoor propagation modelling," in *Proc. ICAP'95*, Eindhoven, Netherlands, Apr. 1995, pp. 231–235.
- [15] C. Gustafson, K. Haneda, S. Wyne and F. Tufvesson, "On mm-wave multi-path clustering and channel modeling," *IEEE Trans. Antennas Propag.*, vol. 62, no. 3, pp.1445–1455, Mar. 2014.
- [16] T. S. Rappaport, *Wireless Communications: Principles and Practice*, Prentice Hall PTR, Upper Saddle River, NJ, USA, 2nd edition, 2002.
- [17] S. Y. Lim, Z. Yun and M. F. Iskander, "Propagation Measurement and Modeling for Indoor Stairwells at 2.4 and 5.8 GHz," *IEEE Trans. Antennas Propag.*, vol. 62, no. 9, pp. 4754–4761, Sept. 2014.
- [18] J. L. Rodgers and W. A. Nicewander, "Thirteen ways to look at the correlation coefficient," *The American Statistician*, vol. 42, pp. 59–66, 1988.
- [19] M. Gudmundson, "Correlation model for shadow fading in mobile radio systems," *IET Electron. Lett.*, vol. 27, no. 23, pp. 2145–2146, Nov. 1991.
- [20] Fraunhofer Heinrich Hertz Institute, "Quasi Deterministic Radio Channel Generator User Manual and Documentation," Jun. 2019.
- [21] S. A. Saputro and J. Chung, "An improved method for estimating antenna correlation coefficient of lossy MIMO arrays," in *Proc. URSI AP-RASC'16*, Seoul, Aug. 2016, pp. 177–180.